ChemCatChem

Research Article
doi.org/10.1002/cctc.202300162

Chemistry Europe
European Chemical Societies Publishing

www.chemcatchem.org

Special Collection

Chemo-Enzymatic One-Pot Oxidation of Cyclohexane via in-situ H_2O_2 Production over Supported AuPdPt Catalysts

Alex Stenner[+],[a] Richard J. Lewis[+],*[a] Joseph Brehm,[a] Tian Qin,[b] Ángeles López-Martín,[a] David J. Morgan,[a, c] Thomas E. Davies,[a] Liwei Chen,[b] Xi Liu,*[b] and Graham J. Hutchings*[a]

The introduction of dopant concentrations of Pt into supported AuPd nanoparticles, when used in conjunction with an evolved unspecific peroxygenase (UPO) from *Agrocybe aegerita* (PaDa-I) is demonstrated to offer high efficacy towards the one-pot selective oxidation of cyclohexane to KA oil (cyclohexanol and cyclohexanone), via the in-situ synthesis of H_2O_2. The optimised AuPdPt/TiO_2/PaDa-I system achieves significant improvements over analogous AuPd or Pd-only formulations or the use of commercially available H_2O_2, with this attributed to the increased rate of H_2O_2 production by the chemo-catalyst, which results from the electronic modification of Pd species via Pt incorporation, upon the formation of trimetallic nanoalloys.

Introduction

Selective C–H bond activation is widely considered a major challenge of chemical feedstock valorisation, with many heterogeneous catalysts suffering from a combination of poor regioselectivity and activity to over-oxidation. For example, the industrial oxidation of cyclohexane to cyclohexanol and cyclohexanone (collectively KA oil), which are key precursors to Nylon-6 and Nylon-6,6 respectively, is typically operated at low conversion rates (approximately 5–10%) to inhibit overoxidation of the desired products.[1–3] Although, even at such moderate rates a substantial concentration of ring-opened by-products, such as 6-hydroxyhexanoic and glucaric acids can be produced.[4]

A number of enzymatic approaches have been developed that do not suffer from the shortcomings associated with chemo-catalytic routes to the selective oxidation of C–H bonds. These include the use of unspecific peroxygenases (UPOs), heme-thiolate enzymes of fungal origins, which are able to utilise H_2O_2 to functionalise C–H bonds with high stereo- and chemo-selectivity.[5] However, a major concern associated with UPOs is their sensitivity to H_2O_2 concentration, rapidly deactivating in the presence of even moderate concentrations of the oxidant.[6] While the utilisation of preformed H_2O_2 may seem attractive, continually supplying the oxidant from an external reservoir would necessitate the continual monitoring of the reaction solution to ensure enzyme stability is retained and would clearly lead to the continual dilution of synthesised products, while the presence of halide and acidic stabilisers, typically found in performed H_2O_2,[7] may represent a potential source of enzyme deactivation, with additional costs associated with their removal from product streams prior to shipping.

As such numerous systems have been developed to supply in-situ synthesised H_2O_2 to UPOs, these include the use of enzymatic cascades, with the use of glucose oxidase (GO_X), formate oxidase (FOx) or choline oxidase (ChOx) co-enzymes previously reported.[8–11] However, such approaches so far have been hampered by poor atom efficiency and the formation of undesirable by-products.[12]

Recently, we have demonstrated that it is possible to couple in-situ H_2O_2 generation, over supported bimetallic Pd-based nanoparticles with the laboratory-evolved UPO from *Agrocybe aegerita*, referred to as PaDa-I, to achieve selective C–H bond activation.[13,14] However, for a chemo-enzymatic approach to be competitive with current industrial technologies there is a need to improve process efficiency with the supply of H_2O_2 from the chemo-catalyst to the UPO a clear rate determining step which limits overall process efficiency.

The alloying of Pd with a range of secondary metals,[15–18] particularly Au,[19–22] has been extensively studied and demonstrated to improve catalytic reactivity and selectivity towards H_2O_2 synthesis when studied under optimised reaction conditions. These enhancements are often attributed to the

[a] *A. Stenner,[+] Dr. R. J. Lewis,[+] J. Brehm, Dr. Á. López-Martín, Dr. D. J. Morgan, Dr. T. E. Davies, Prof. G. J. Hutchings*
Max Planck-Cardiff Centre on the Fundamentals of Heterogeneous Catalysis FUNCAT
Cardiff Catalysis Institute
School of Chemistry
Cardiff University
Cardiff, CF10 3AT (UK)
E-mail: LewisR27@Cardiff.ac.uk
Hutch@Cardiff.ac.uk
[b] *T. Qin, Prof. L. Chen, Prof. X. Liu*
In-situ Centre for Physical Sciences
School of Chemistry and Chemical
Frontiers Science Centre for Transformative Molecules
Shanghai 200240 (P. R. China)
E-mail: LiuXi@edu.cn
[c] *Dr. D. J. Morgan*
HarwellXPS
Research Complex at Harwell (RCaH)
Didcot, OX11 OFA (UK)
[+] *These authors contributed equally to this work.*

Supporting information for this article is available on the WWW under https://doi.org/10.1002/cctc.202300162

This publication is part of a Special Collection on "Heterogeneous Chemo-Enzymatic Catalysis". Please check the ChemCatChem homepage for more articles in the collection.

modification of Pd oxidation states and the disruption of contiguous Pd domains.[23] In recent years growing interest has been placed on the introduction of metal dopants into mono- and bi-metallic systems both for the direct synthesis of H_2O_2[24] and a range of selective transformations,[25,26] with the incorporation of low levels of Pt into supported Pd[27,28] and AuPd[29,30] species in particular shown to enhance catalytic performance far beyond that observed over parent materials.

With these earlier studies in mind and with an aim to further improve overall process efficiency, we now investigate the efficacy of Pt introduction, at dopant concentrations, into supported AuPd nanoparticles when used in conjunction with PaDa-I for the selective oxidation of cyclohexane to KA oil. A proposed reaction scheme for the combined chemo-catalytic/enzymatic approach to cyclohexane valorisation is reported in Figure 1.

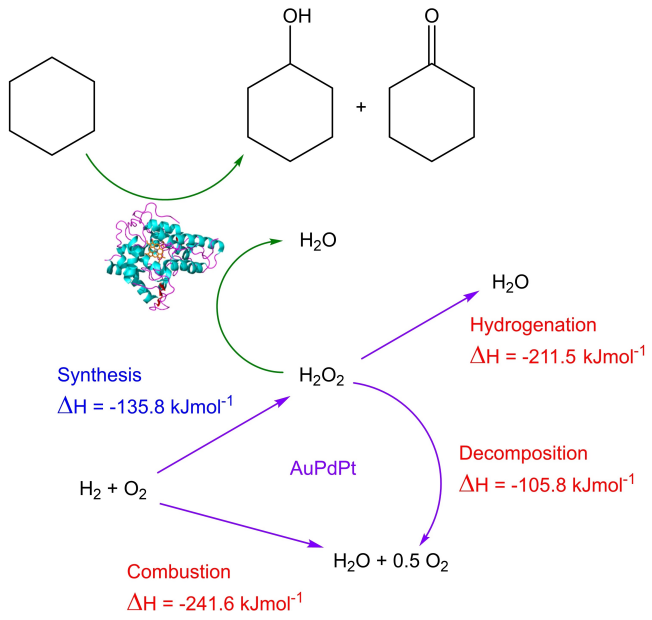

Figure 1. Proposed reaction pathways associated with the chemo-catalytic/enzymatic valorisation of cyclohexane. ***Key:*** Chemo-catalytic pathways (*purple*), enzymatic pathways (*green*).

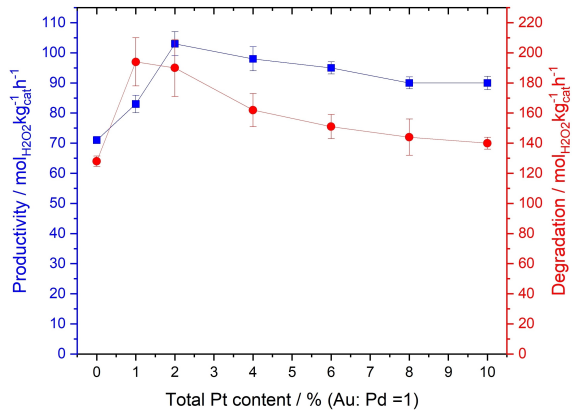

Figure 2. Catalytic activity of 1%AuPdPt/TiO_2 catalysts towards the direct synthesis and degradation of H_2O_2, under high-pressure batch conditions, as a function of Pt content. **H_2O_2 direct synthesis reaction conditions**: Catalyst (0.01 g), H_2O (2.9 g), MeOH (5.6 g), 5% H_2/CO_2 (420 psi), 25% O_2/CO_2 (160 psi), 0.5 h, 2 °C, 1200 rpm. **H_2O_2 degradation reaction conditions**: Catalyst (0.01 g), H_2O_2 (50 wt.% 0.68 g) H_2O (2.22 g), MeOH (5.6 g), 5% H_2/CO_2 (420 psi), 0.5 h, 2 °C, 1200 rpm.

Results and Discussion

Our initial studies established the efficacy of a range of supported Pd-based catalysts, prepared by a conventional wet co-impregnation procedure, towards the direct synthesis and subsequent degradation of H_2O_2 (Figure 2, with catalytic selectivity towards H_2O_2 and H_2 conversion rates reported in Table S1, and the performance of mono- and bi-metallic analogues reported in Table S2). These experiments were carried out under high-pressure batch reaction conditions, which have previously been optimized to enhance H_2O_2 stability, namely through the presence of an alcohol co-solvent (in this case methanol) and a CO_2 gaseous diluent (which forms carbonic acid in-situ, lowering pH of the reaction solution), both of which have been shown to inhibit H_2O_2 degradation to H_2O.[31] While these conditions are clearly not suitable for an enzymatic approach to cyclohexane oxidation they are considered to allow for variation in catalytic performance towards the direct synthesis of H_2O_2 to be more easily discerned.

In keeping with numerous previous studies,[32–34] the alloying of Au with Pd, was found to considerably enhance catalytic performance with the 0.5%Au-0.5%Pd/TiO_2 formulation offering both a greater rate of H_2O_2 synthesis (71 mol$_{H2O2}$ kg$_{cat}^{-1}$ h^{-1}) and improved selectivity towards H_2O_2 as supported by determination of H_2O_2 degradation rates (128 mol$_{H2O2}$ kg$_{cat}^{-1}$ h^{-1}), compared to that achieved by the monometallic Pd analogue (56 and 139 mol$_{H2O2}$ kg$_{cat}^{-1}$ h^{-1} for H_2O_2 synthesis and degradation pathways respectively). Such improvements have been previously attributed to the ability of Au to both electronically modify Pd speciation and disrupt the formation of contiguous Pd ensembles.[35,36] Notably in the case of AuPd-based catalysts exposed to an oxidative heat treatment, such as in this study, the formation of nanoparticles consisting of Au-core, Pd-shell morphologies has been widely reported to be a key feature responsible for the observed improved selectivity, particularly when immobilising metal nanoparticles onto oxide supports.[37]

The introduction of Pt into the AuPd formulation, at dopant concentrations (0.01–0.02 wt.%), was found to considerably improve catalytic performance, with rates of H_2O_2 synthesis achieved by the 0.49%Au-0.49%Pd-0.02%Pt/TiO_2 catalyst particularly noteworthy (104 mol$_{H2O2}$ kg$_{cat}^{-1}$ h^{-1}), with such observations aligning well with our previous studies into similar systems.[30,38] However, such an improvement cannot be ascribed to an increase in catalytic selectivity, with the 0.49% Au-0.49%Pd-0.02%Pt/TiO_2 catalyst offering degradation rates (190 mol$_{H2O2}$ kg$_{cat}^{-1}$ h^{-1}) considerably greater than the AuPd analogue (128 mol$_{H2O2}$ kg$_{cat}^{-1}$ h^{-1}). These observations were found to align well with our determination of H_2 selectivity during the H_2O_2 synthesis reaction (Table S1), although it should

be noted that such comparisons were not made at iso-conversion, with the rate of H_2 conversion over the 0.49%Au-0.49%Pd-0.02%Pt/TiO_2 catalyst (38%) more than double that of the bimetallic formulation (16%). In keeping with earlier studies the further introduction of Pt (*i.e.* 0.02–0.1 wt.%) was found to lead to a loss in catalytic performance,[30] although all trimetallic formulations outperformed both the Pd-only and AuPd analogues, regardless of Pt content.

Building on these initial studies we next evaluated catalytic performance towards the direct synthesis and subsequent degradation of H_2O_2, under conditions considered suitable for C–H bond activation when utilising the chemo-enzymatic cascade system, namely at ambient temperature, low pressure (29 psi) and using a phosphate-buffered reaction medium (pH 6),[39] with catalytic performance after a reaction time of 5 and 120 min reported in Table 1. Notably in the case of the H_2O_2 degradation experiments concentrations of H_2O_2 (2000 ppm) far greater than those generated in the analogous H_2O_2 synthesis experiments were required in order to clearly distinguish trends in catalytic performance. While a comparison of net H_2O_2 concentrations achieved over a standard 2 h reaction suggests there is a limited difference in catalytic performance across the 1%AuPdPt/TiO_2 series it is important to note that for application in the chemo-enzymatic cyclohexane oxidation reaction, any H_2O_2 generated over the chemo-catalyst will be readily utilised by the enzyme for selective C–H bond activation. As such a comparison of initial reaction rates of H_2O_2 synthesis, where the contribution from competitive H_2O_2 degradation pathways is considered minimal, may be considered a more accurate indication of catalytic performance when the chemo-catalyst is utilised in tandem with PaDa-I, for cyclohexane oxidation. Interestingly determination of initial rates of H_2O_2 synthesis, under conditions favourable to enzyme stability, align well with trends identified using high-pressure reaction conditions and would identify the 0.5%Au-0.5%Pd/TiO_2 and 0.49%Au-0.49%Pd-0.02%Pt/TiO_2 catalysts as choice candidates for application in the chemo-enzymatic cascade.

Subsequently, we investigated the efficacy of the chemo-catalyst formulations, when used in tandem with PaDa-I, towards the selective oxidation of cyclohexane to the corresponding alcohol and ketone (KA oil) via in-situ H_2O_2 production (Figure 3, with a comparison of reaction rates reported in Table S3). Perhaps expectedly given the observed synergy often reported through the alloying of Pd with Au the 0.5%Au-0.5%Pd/TiO_2 catalyst was found to offer higher activity towards cyclohexane oxidation, when used in conjunction with PaDa-I (17.4% cyclohexane conversion) than the monometallic Pd analogue (14.5% cyclohexane conversion). Notably, such a trend may have been predicted based on our determination of initial rates of H_2O_2 synthesis under comparable reaction conditions (Table 1).

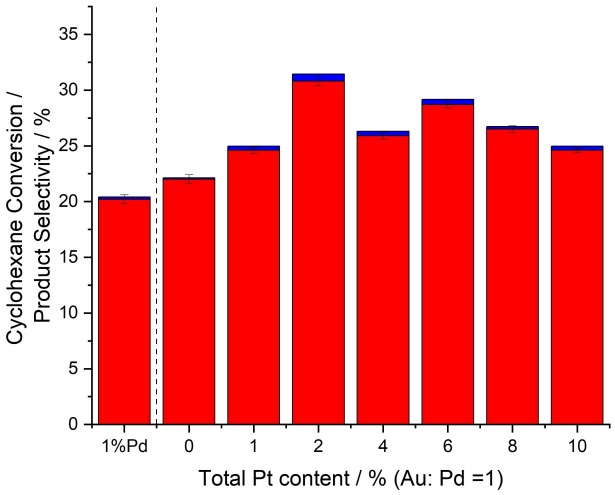

Figure 3. Catalytic activity of 1%AuPdPt/TiO_2 catalysts towards the selective oxidation of cyclohexane in conjunction with PaDa-I, as a function of Pt content. ***Key:*** cyclohexanol (*red*), cyclohexanone (*blue*). **Cyclohexane oxidation reaction conditions:** Catalyst (0.001 g), cyclohexane (10 mM), PaDa-I (15 U mL_{RM}^{-1}), phosphate buffer (10 mL, pH 6.0), using a gas mixture of 80% H_2/air H_2 (23 psi) and air (6 psi), 2 h, 20 °C, 250 rpm.

Upon the introduction of dopant concentrations of Pt into the AuPd catalyst, a significant improvement in cyclohexanone conversion was observed, with an optimal catalyst formulation identified (0.49%Au-0.49%Pd-0.02%Pt/TiO_2), which offered cyclohexane conversion rates approximately 1.5 times greater (25.7% cyclohexane conversion) than that achieved by the bimetallic analogue, again such trends may have been predicted based on H_2O_2 synthesis rates. With the further introduction of Pt, cyclohexane conversion rates decreased

Table 1. Comparison of catalytic activity towards the direct synthesis and subsequent degradation of H_2O_2, under low-pressure conditions.

	Reaction rate [$mmol_{H2O2}^{-1}$ $mmol_{metal}$ h^{-1}]		
	5 min	120 min	
Catalyst	H_2O_2 synthesis	H_2O_2 synthesis	H_2O_2 degradation
1%Pd/TiO_2	3.00×10^{2}	4.0×10^{1}	6.50×10^{1}
0.5%Au-0.5%Pd/TiO_2	5.36×10^{2}	5.54×10^{1}	1.19×10^{2}
0.495%Au-0.495%Pd-0.01%Pt/TiO_2	5.62×10^{2}	1.42×10^{1}	7.87×10^{1}
0.49%Au-0.49%Pd-0.02%Pt/TiO_2	6.13×10^{2}	3.02×10^{1}	5.27×10^{1}
0.48%Au-0.48%Pd-0.04%Pt/TiO_2	5.08×10^{2}	7.24×10^{1}	5.88×10^{1}
0.47%Au-0.47%Pd-0.06%Pt/TiO_2	4.55×10^{2}	2.97×10^{1}	5.59×10^{1}
0.46%Au-0.46%Pd-0.08%Pt/TiO_2	4.74×10^{2}	1.72×10^{1}	5.07×10^{1}
0.45%Au-0.45%Pd-0.1%Pt/TiO_2	3.92×10^{2}	0.79×10^{1}	5.10×10^{1}

H_2O_2 direct synthesis reaction conditions: catalyst (0.001 g), phosphate buffer (100 mM, 10 mL, pH 6.0), using a gas mixture of 80% H_2/air (23 psi H_2, 6 psi air), 20 °C, 250 rpm. **H_2O_2 degradation reaction conditions**: Catalyst (0.001 g), H_2O_2 (2000 ppm), phosphate buffer (100 mM, 10 mL, pH 6.0), using a gas mixture of 80% H_2/air H_2 (23 psi) and N_2 (6 psi), 20 °C, 250 rpm.

considerably, however for all formulations studied near total selectivity towards cyclohexanol was observed (≥98% cyclohexanol selectivity).

The catalytic activity of immobilised Pd-based catalysts towards H_2O_2 production is known to be highly dependent on Pd speciation, with Pd^{2+} species typically more selective towards H_2O_2 than Pd^0 analogous. Although, a growing number of studies have highlighted the improved efficacy of mixed domains of Pd^0-Pd^{2+}, compared to Pd^0- or Pd^{2+}-rich counterparts. Regardless, given the rapid utilisation of H_2O_2 in the enzyme-mediated selective oxidation of cyclohexane, it may be reasoned that chemo-catalytic H_2O_2 degradation pathways are of limited concern, with respect to overall process efficiency. On this basis, one could recommend future chemo-catalyst design should focus on the development of materials which are highly active towards H_2O_2 production, even if such improvements were at the expense of catalytic selectivity, with the caveat that the reaction remains limited by the supply of H_2O_2 by the chemo-catalyst, rather than its subsequent utilisation in selective oxidation. Analysis of the 1%AuPdPt/TiO_2 catalyst series via X-ray photoelectron spectroscopy (XPS) (Figure 4) indicated that Pd is present predominantly as Pd^{2+}in the case of the 1%Pd/TiO_2 catalyst, which is perhaps understandable given the exposure to an oxidative heat treatment (flowing air, 400 °C, 3 h) and the preferential formation of PdO. Notably, upon the alloying of Pd with Au and the subsequent introduction of dopant levels of Pt a further shift towards Pd^{2+} was observed, although such a shift may be considered relatively minor, it does highlight the electronic modification which may be achieved through the formation of nanoalloys.

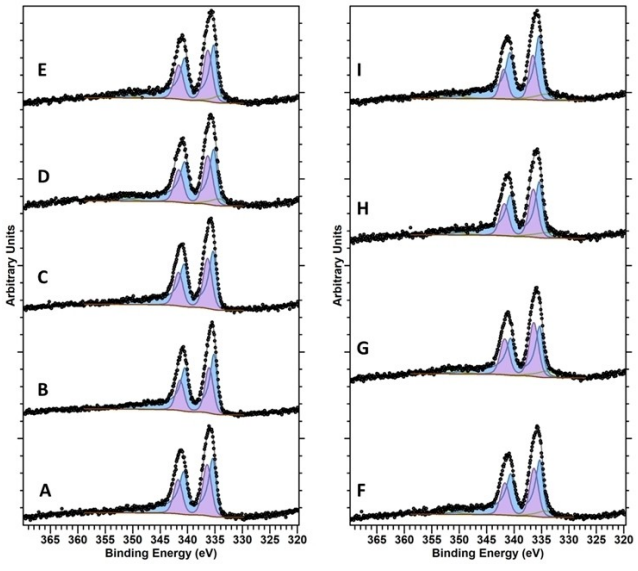

Figure 4. Surface atomic compositions of as-prepared catalysts, prepared via a conventional wet co-impregnation excess chloride impregnation methodology, as a function of secondary metal modifier, as determined by XPS using Pd (3d) regions. **(A)** 0.5%Pd/TiO_2, **(B)** 1%Pd/TiO_2, **(C)** 0.5%Au-0.5%Pd/TiO_2, **(D)** 0.45%Au-0.45%Pd-0.01%Pt/TiO_2, **(E)** 0.495%Au-0.495%Pd-0.02%Pt/TiO_2, **(F)** 0.48%Au-0.48%Pd-0.04%Pt/TiO_2, **(G)** 0.47%Au-0.47%Pd-0.06%Pt/TiO_2, **(H)** 0.46%Au-0.46%Pd-0.08%Pt/TiO_2, **(I)** 0.45%Au-0.45%Pd-0.1%Pt/TiO_2. ***Key***: Au^0 (*green*), Pd^0 (*blue*), Pd^{2+} *i.e.* PdO (*purple*).

However, it should be noted that the Pd speciation of the fresh materials are likely to not be representative of the as-prepared materials, in particular given the large concentrations of H_2 utilised within the chemo-enzymatic cascade system.

With our analysis by XPS indicating both the effect of AuPd alloy formation and the subsequent introduction of dopant levels of Pt on Pd speciation (Figure 4) we subsequently probed the series of catalysts via CO-DRIFTS (Figure S1). The DRIFTS spectra of all formulations was found to be dominated by Pd-CO bands, associated with the bridged and multi-fold adsorption of CO on extended Pd surfaces (1750–2000 cm^{-1}).[34] Indeed, there is no clear indication of CO bonded to low-coordination Pd sites (*i.e.* edge and corner sites), which would be expected at high wavenumbers (>2000 cm^{-1}),[34] such observations may indicate the limited presence of highly dispersed Pd species (*i.e.* atoms or clusters), which is typical of the wet impregnation route to catalyst synthesis.[40] Upon the alloying of Pd with Au a clear blueshift in the bands associated with bridging/multi-fold CO species was observed, which aligns well with previous reports by Wilson *et al.* and can be attributed to the occupation of lower coordination sites.[41] Additionally, a near-total loss in the intensity of the band centred at approximately 1795 cm^{-1} was detected, which is characteristic of a substantial modification of Pd surface structures, resulting from the formation of AuPd alloyed species.[42] Notably, the subsequent introduction of Pt at low concentrations was not found to result in any detectable variation in structural motifs, which may be expected given the loadings of the individual metals. However, for those formulations with relatively high concentrations of Pt (≥0.06 wt.%), bands associated with CO coordinated to Pt domains may be observed.[43]

We subsequently established the significant improvement in selective cyclohexane oxidation activity that can be achieved via the in-situ production of H_2O_2, in comparison to that observed when either gaseous reagent (H_2 and O_2 (as air)) is used separately (Table S4). Interestingly significantly higher rates of cyclohexane conversion were achieved via the in-situ production of H_2O_2 (17.4%) compared to that obtained when using the preformed oxidant (0.8–4.6% cyclohexane conversion at H_2O_2 concentrations ranging from 50–200 ppm) at comparable concentrations to that generated by the chemo-catalyst and under analogous reaction conditions to those used for the selective oxidation of cyclohexane. This can be understood to be related at least in part, to the complete addition of the oxidant at the start of the reaction and the susceptibility of the PaDa-I enzyme to high concentrations of H_2O_2, with the mechanism of deactivation considered to occur through the loss of the heme-centre, precipitated by the generation of highly reactive oxygen-based radicals (in particular $^{\bullet}OH$ and $^{\bullet}OOH$) via the reaction of H_2O_2 with UPO compound III.[44]

Using an ABTS assay we next determined the contribution of key reaction parameters towards enzyme deactivation (Table S5). A considerable loss in enzyme activity was observed after exposure to in-situ reaction conditions (approximately 18%), with the presence of the organic substrate and major product (at a concentration comparable to that generated during the chemo-catalytic/enzymatic cascade) found to con-

tribute significantly toward enzyme deactivation (23 and 25% reduction in activity observed in the presence of cyclohexane and cyclohexanol respectively). The introduction of preformed H_2O_2 at concentrations comparable to that generated over the chemo-catalyst (50 ppm) led to a major loss in enzyme activity (approximately 68% reduction), with a direct correlation between H_2O_2 concentration and the extent of enzyme deactivation observed. These studies align well with our earlier investigations (Table S4), where limited cyclohexane oxidation activity was observed in the presence of the preformed oxidant, and the known sensitivity of the UPOs to H_2O_2 concentration, as discussed above.

With a particular focus on the 1%Pd/TiO_2, 0.5%Au-0.5%Pd/TiO_2 and 0.49%Au-0.49%Pd-0.02%Pt/TiO_2 catalysts time-on-line studies were next conducted (Figure 5). As with our standard reaction time (2 h) the higher activity of the optimal AuPdPt formulation is once again clear, with rates of cyclohexane conversion (58%) far greater than that of either the 0.5%Au-0.5%Pd/TiO_2 (43%) or 1%Pd/TiO_2 (39%) catalysts, over extended reaction times (8 h). Notably, selectivity towards cyclohexanol remained high in all cases. We subsequently set out to determine the contribution of a purely chemo-catalytic pathway to cyclohexanol over-oxidation to the corresponding ketone (Figure S2) and while it was identified that such a route is possible, it is clear that the enzymatic contribution to over-oxidation is far greater.

With the potential for the long-term deactivation of the enzyme as a result of interaction with leached metal species, we next conducted model studies in order to determine the extent of precious metal leaching over 8 h of reaction (Table S6). Such studies were conducted in the absence of both the PaDa-I enzyme and the cyclohexane substrate and at catalyst loadings (0.01 g) ten times greater than that utilised for our standard low-pressure H_2O_2 direct synthesis studies, in order to allow for more accurate determination of metal concentrations. Notably, for the three catalyst formulations studied no metal leaching was observed. Building on these initial studies we conducted further model cyclohexane oxidation experiments, in order to determine the role of immobilised metal species on enzyme stability. These experiments were conducted in the presence of the PaDa-I enzyme and using concentrations of metal species (as chloride salts) equivalent to that which would be present if 0.1% of metal species were leached from monometallic 1%Au/TiO_2, 1%Pd/TiO_2 and 1%Pt/TiO_2 catalysts, again using a catalyst mass ten times that utilised for our standard cascade reactions (*i.e.* 0.01 g). ABTS assay experiments revealed the potential for significant deactivation of the PaDa-I enzyme after exposure to metal salts, in particular when the enzyme was exposed to Pt (as H_2PtCl_6), which resulted in a near total loss of enzymatic activity (Table S7), with additional control experiments indicating the negligible effect of the chloride counter ion. While such observations clearly highlight the detrimental effect of leached metal species on enzyme stability and should inform future studies, it should again be highlighted that we observe no metal leaching of active metals under model reaction conditions.

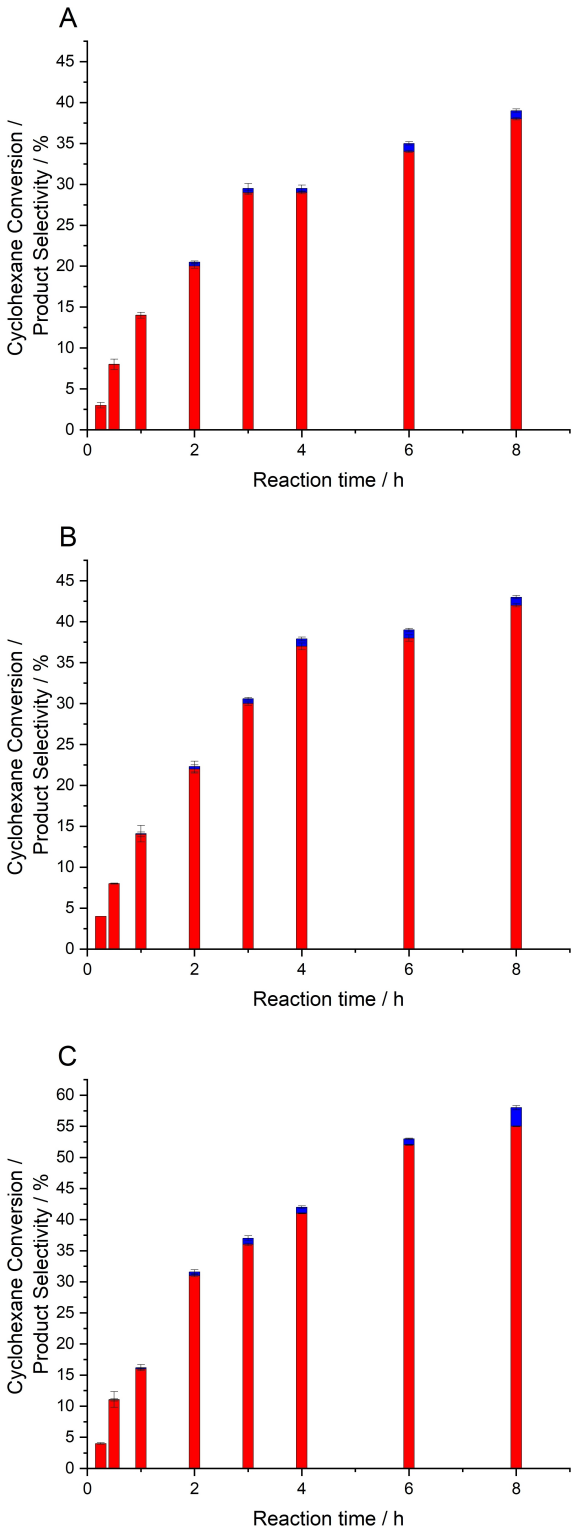

Figure 5. Comparison of catalytic activity of **(A)** 1%Pd/TiO_2, **(B)** 0.5%Au-0.5%Pd/TiO_2 and **(C)** 0.49%Au-0.49%Pd-0.02%Pt/TiO_2 when used in conjunction with PaDa-I towards the selective oxidation of cyclohexane, as a function of reaction time. ***Key***: cyclohexanol (*red*), cyclohexanone (*blue*). **Cyclohexane oxidation reaction conditions**: Catalyst (0.001 g), cyclohexane (10 mM), PaDa-I (15 U mL_{RM}^{-1}), phosphate buffer (10 mL, pH 6.0), using a gas mixture of 80% H_2/air H_2 (23 psi) and air (6 psi), 20 °C, 250 rpm.

Further investigation of the 1%Pd/TiO_2, 0.5%Au-0.5%Pd/TiO_2 and 0.49%Au-0.49%Pd-0.02%Pt/TiO_2 catalysts via STEM-HAADF imaging indicated a considerable variation in nanoparticle size with catalyst formulation (Figures 6–7). As previously reported for analogous materials,[45] the Pd-only catalyst was found to consist of small (< 2 nm) nanoparticles, we should again highlight our analysis by CO-DRIFTS, which indicated the lack of any sub-nano Pd species (Figure S1). Upon the introduction of Au a population of larger (> 5 nm) nanoparticles were observed in addition to the smaller species identified in the Pd-only analogue. XEDS mapping of individual nanoparticles revealed that the smaller species consisted of Pd only, whereas the larger particles were Au-rich alloys. In a similar manner to the bimetallic AuPd catalyst, the 0.49%Au-0.49%Pd-0.02%Pt/TiO_2 analogue also displayed a wide particle size range, with the smaller Pd-only particles observed in addition to AuPdPt nanoalloys. Additional HAADF-STEM and XEDS analysis of the 0.5%Au-0.5%Pd/TiO_2 and 0.49%Au-0.49%Pd-0.02%Pt/TiO_2 catalysts are reported in Figures S3 and S4 and in particular, we wish to highlight the XEDS analysis of the individual nanoparticles within the trimetallic catalyst which further demonstrates the formation AuPdPt nanoalloys.

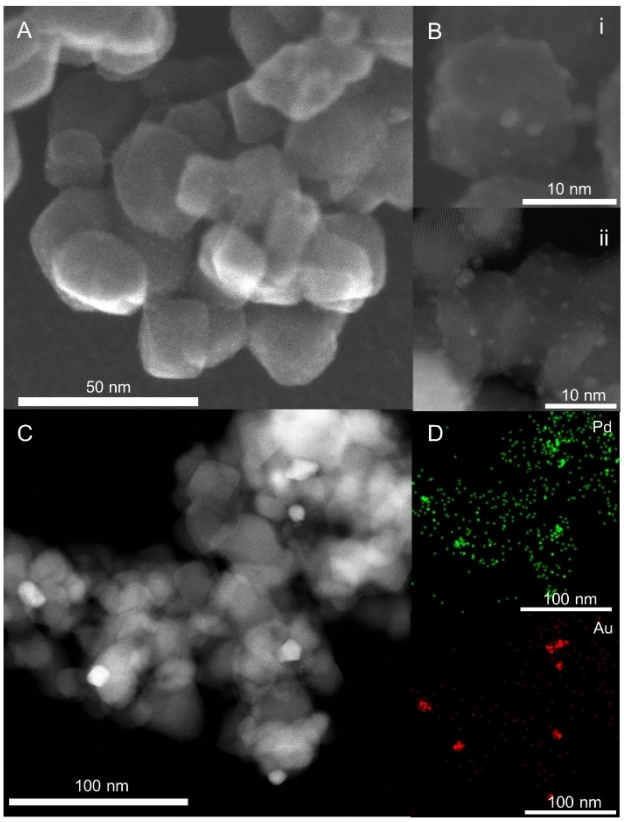

Figure 6. HAADF-STEM and X-EDS imaging of the as-prepared 1%Pd/TiO_2 and 0.5%Pd-0.5%Au/TiO_2 catalysts. **(A)** Lower magnification of 1%Pd/TiO_2 showing the absence of larger particles, **(B)** high-magnification images of 1%Pd/TiO_2 from areas indicated showing small (≤ 3 nm) Pd clusters on TiO_2 surface, **(C)** analysis of the 0.5%Pd-0.5%Au/TiO_2 catalyst showing both small and larger (5–20 nm) nanoparticles, and **(D)** Pd and Au X-EDS maps of the area in **(C)** showing the presence of Au–Pd nanoalloys. Additional analysis of the 0.5%Pd–0.5%Au/TiO_2 catalyst is reported in Figure S3.

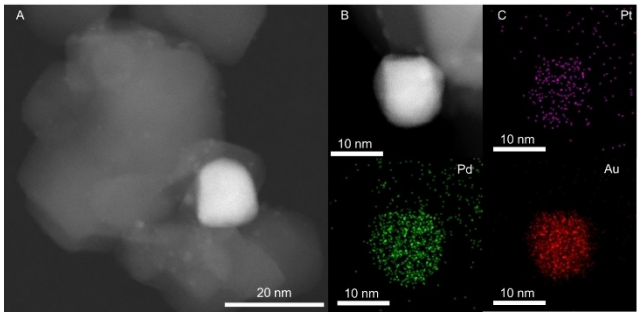

Figure 7. HAADF-STEM and X-EDS imaging of the as-prepared 0.49%Pd–0.49%Au-0.02%Pt/TiO_2 catalyst. **(A)** Lower magnification image showing the presence of both small (≤ 3 nm) and larger particles (> 10 nm) nanoparticles, **(B)** high-magnification images again indicating the presence of larger nanoparticles on the TiO_2 surface, **(C)** Pt, Pd and Au X-EDS maps of area in **(B)** showing the presence of Au–Pd-Pt nanoalloys. Additional analysis of the 0.49%Pd-0.49%Au-0.02%Pt/TiO_2 catalyst is reported in Figure S4.

Finally, with the requirement for catalyst stability of the utmost importance we next evaluated catalytic performance towards the tandem chemo-catalytic/enzymatic oxidation of cyclohexane over multiple uses (Table S8), notably fresh enzyme was utilised for each reaction. Interestingly, for all catalysts studied performance was found to improve considerably over three successive reactions, with further studies indicating a similar general improvement in catalytic activity towards the direct synthesis, under comparable reaction conditions and at a reaction time where H_2O_2 degradation pathways can be considered to be negligible (Table S8). While these two metrics (chemo-catalyst driven H_2O_2 synthesis and subsequent utilisation by PaDa-I in the oxidation of cyclohexane) are clearly related we were motivated to gain further understanding of the underlying cause of such an improvement. Analysis of the three key catalysts after successive use in the oxidation of cyclohexane via XPS revealed a significant reduction in Pd^{2+} content upon use in the chemo-enzymatic selective oxidation of cyclohexane (Figure S5), with the limited presence of Pd^{2+} attributed to the oxidation of the catalyst surface upon drying and handling during ambient conditions prior to analysis. As such it is possible to attribute the in-situ reduction of Pd^{2+} species as the cause for the improved performance in the chemo-catalytic/enzymatic oxidation of cyclohexane. As discussed previously, we consider that such observations will aid in the design of more active chemo-catalysts and in the development of more efficient cascade systems.

Conclusion and Future Perspective

The combination of H_2O_2 synthesising chemo-catalyst and unspecific peroxygenase enzyme, PaDa-I, offers an attractive route to the selective oxidation of cyclohexane to the corresponding alcohol and ketone (collectively KA oil). However, significant improvements in process efficiency are required if the chemo/enzymatic cascade is to rival current industrial technologies. In particular, there is a clear need to

maximise H_2O_2 synthesis rates, while ensuring that the rate of production does not exceed that which the enzymatic component is able to selectively utilise in C–H bond activation. Indeed, an overproduction of H_2O_2, is clearly detrimental to enzyme stability, with additional costs associated with non-selective H_2 utilisation.

Through the introduction of dopant concentrations of Pt into supported AuPd nanoparticles and the subsequent electronic modification of Pd species, we demonstrate that it is possible to achieve significantly enhanced product yields, compared to those observed over the parent bimetallic formulation, with no loss over key chemo-catalytic formulations upon successive use. Such improvements both upon Pt incorporation and catalyst re-use can be directly related to the improved activity of the chemo-catalyst towards H_2O_2 production.

We have also identified the potential for enzymatic deactivation under cascade reaction conditions and as a result of interaction with metals responsible for H_2O_2 synthesis, although no such metal leaching was observed when using key formulations. We consider such observations will aid in further process design and optimisation.

However, while the benefits of the chemo-catalytic/enzymatic approach are clear one must also consider the industrial feasibility of such systems, in particular given the limited stability of the free enzyme, both under operational conditions and during separation stages.[46] It is well known that the use of immobilised enzymes can offer operational advantages, improving stability under non-optimal reaction parameters (temperature, pH or the use of organic solvents), while also reducing purification and separation steps associated with the free enzyme.[47,48] Indeed, the use of so-called natural heterogeneous catalysts,[49] alongside traditional chemo-catalysts would allow for the adoption of continuous/semi-continuous reactor systems.[46] It is recommended that future studies focus on the use of such immobilised systems as a matter of priority.

Experimental

Mono-, bi- and tri-metallic 1%AuPdPt/TiO_2 catalysts have been prepared (on a weight basis) via a conventional wet co-impregnation procedure, based on a methodology previously reported in the literature.[29] The procedure to produce the 0.49%Au-0.49%Pd-0.02%Pt/TiO_2 catalyst (2 g) is outlined below, with a similar methodology utilized for all formulations. Exact quantities of catalyst precursors are reported in Table S9.

Aqueous solutions of $PdCl_2$ (0.70 mL, [Pd] = 7.0 mg mL^{-1}, Merck), $HAuCl_4 \cdot 3H_2O$ solution (0.445 mL, [Au] = 12.25 mg mL^{-1}, Strem Chemicals) and $H_2PtCl_6 \cdot 6H_2O$ (0.20 mL, [Pt] = 1.0 mg mL^{-1}, Merck) were mixed in a 50 mL round-bottom flask and heated to 65 °C with stirring (1000 rpm) in a thermostatically controlled oil bath, with total volume fixed to 16 mL using H_2O (HPLC grade, Fischer Scientific). Upon reaching 65 °C, TiO_2 (1.98 g, Degussa, P25) was added over the course of 5 min with constant stirring. The resulting slurry was stirred at 65 °C for a further 15 min, following this the temperature was raised to 95 °C for 16 h to allow for complete evaporation of water. The resulting solid was ground prior to an oxidative heat treatment (flowing air, 400 °C, 3 h, 10 °C min^{-1}).

Surface area measurements of key catalytic materials, as determined by five-point N_2 adsorption are reported in Table S10. Corresponding analysis by X-ray diffraction is reported in Figure S6, with no reflections associated with immobilised metals observed, which may be indicative of the high dispersion of metal species.

Catalyst Testing

Note 1: In all cases, reactions were run multiple times, over multiple batches of catalyst, with the data being presented as an average of these experiments.

Note 2: Reaction conditions used within this study operate outside the flammability limits of gaseous mixtures of H_2 and O_2.

Note 3: The conditions used within this work for H_2O_2 synthesis and degradation using high-pressure batch conditions have previously been investigated, with the presence of CO_2 as a diluent for reactant gases and a methanol co-solvent in the case of the high-pressure experiments identified as key to maintaining high catalytic efficacy towards H_2O_2 production.[31]

Direct synthesis of H_2O_2 from H_2 and O_2, under high-pressure batch conditions

Hydrogen peroxide synthesis was evaluated using a Parr Instruments stainless steel autoclave with a nominal volume of 100 mL, equipped with a PTFE liner and a maximum working pressure of 2000 psi. To test each catalyst for H_2O_2 synthesis, the autoclave liner was charged with catalyst (0.01 g) and HPLC grade solvents (5.6 g methanol and 2.9 g H_2O, both Fischer Scientific). The charged autoclave was then purged three times with 5%H_2/CO_2 (100 psi) before filling with 5%H_2/CO_2 to a pressure of 420 psi, followed by the addition of 25%O_2/CO_2 (160 psi). Pressures of 5%H_2/CO_2 and 25%O_2/CO_2 are given as gauge pressures and reactant gasses were not continually supplied. The reaction was conducted at a temperature of 2 °C, for 0.5 h with stirring (1200 rpm), with the reactor temperature controlled using a HAAKE K50 bath/circulator using an appropriate coolant.

H_2O_2 productivity and H_2O_2 concentrations (wt.%) were determined by titrating aliquots of the final solution after reaction with acidified $Ce(SO_4)_2$ (0.0085 M) in the presence of ferroin indicator. Catalyst productivities are reported as $mol_{H2O2}\, kg_{cat}^{-1}\, h^{-1}$.

Total autoclave capacity was determined via water displacement to allow for accurate determination of H_2 conversion and H_2O_2 selectivity. When equipped with a PTFE liner, the total volume of an unfilled autoclave was determined to be 93 mL, which includes all available gaseous space within the autoclave.

Catalytic conversion of H_2 and selectivity towards H_2O_2 were determined using a Varian 3800 GC fitted with TCD and equipped with a Porapak Q column.

H_2 conversion [Equation (1)] and H_2O_2 selectivity [Equation (2)] are defined as follows:

$$H_2\text{Conversion}\ (\%) = \frac{\text{mmol}_{\text{H2 (t(0))}} - \text{mmol}_{\text{H2 (t(1))}}}{\text{mmol}_{\text{H2 (t(0))}}} \times 100 \quad (1)$$

$$H_2O_2\ \text{Selectivity}\ (\%) = \frac{H_2O_2\text{detected (mmol)}}{H_2\ \text{consumed (mmol)}} \times 100 \quad (2)$$

Degradation of H_2O_2, under high-pressure batch conditions

Catalytic activity towards H_2O_2 degradation (via hydrogenation and decomposition pathways) was determined in a similar manner to that used to measure the direct synthesis activity of a catalyst. The autoclave liner was charged with methanol (5.6 g, HPLC standard, Fischer Scientific), H_2O_2 (50 wt.%, 0.69 g, Merck), H_2O (2.21 g, HPLC standard, Fischer Scientific) and catalyst (0.01 g), with the solvent composition equivalent to a 4 wt.% H_2O_2 solution. From the solution, prior to the addition of the catalyst, two 0.05 g aliquots were removed and titrated with acidified $Ce(SO_4)_2$ solution using ferroin as an indicator to determine an accurate concentration of H_2O_2 at the start of the reaction. The autoclave was purged three times with 5%H_2/CO_2 (100 psi) before filling with 5%H_2/CO_2 to a gauge pressure of 420 psi. The reaction was conducted at a temperature of 2 °C, for 0.5 h with stirring (1200 rpm). After the reaction was complete the catalyst was removed from the reaction mixture by filtration and two 0.05 g aliquots were titrated against the acidified $Ce(SO_4)_2$ solution using ferroin as an indicator. The degradation activity is reported as $mol_{H2O2}\, kg_{cat}^{-1}\, h^{-1}$.

Direct synthesis of H_2O_2 from H_2 and O_2, under low-pressure batch conditions

Reactions were carried out in 50 mL gas tight round bottomed flasks rated to 60 psi and stirred using a Radleys 6 Plus Carousel equipped with a gas distribution system. The catalyst (0.001 g) was weighed directly into the glass flasks. To this was added potassium phosphate buffer (10 mL of 100 mM, pH 6.0) prepared with KH_2PO_4 and K_2HPO_4 (both obtained from Merck). Subsequently, the flask was sealed and pressurized to 29 psi with H_2 (23 psi) and air (6 psi) to give a reaction atmosphere containing 80% H_2 and 20% air. The reaction mixtures were stirred (250 rpm) at ambient temperature (20 °C) for 0.5 h, unless otherwise stated. After the desired reaction time the vessel was depressurized and the H_2O_2 concentration determined by UV/Vis spectroscopy. To determine H_2O_2 concentration an aliquot (1.5 mL) of the post reaction solution was combined with potassium titanium oxalate dihydrate solution acidified with 30% H_2SO_4 (0.02 M, 1.5 mL) resulting in the formation of an orange pertitanic acid complex. This resulting solution was analysed spectrophotometrically using an Agilent Cary 60 UV/Vis Spectrophotometer at 400 nm by comparison to a calibration curve by taking aliquots of H_2O_2 in the buffer solution (1.5 mL) and adding acidified potassium titanium oxalate dihydrate solution (1.5 mL).

Degradation of H_2O_2, under low-pressure batch conditions

Catalytic activity towards H_2O_2 degradation (via hydrogenation and decomposition pathways) was determined in a similar manner to that used to measure the direct synthesis activity of a catalyst, under low pressure conditions. The potassium phosphate buffer (10 mL of 100 mM, pH 6.0) prepared with KH_2PO_4 and K_2HPO_4 (both obtained from Merck) and H_2O_2 (2000 ppm, Merck) were added into the 50 mL gas-tight round bottomed flasks. From the solution, prior to the addition of the catalyst, two 0.05 g aliquots were removed to allow for the quantification of the initial H_2O_2 concentration via UV/Vis spectroscopy. Subsequently, the catalyst (0.001 g) was added to the flask, which was then sealed, purged and pressurized to 29 psi with H_2 (23 psi) and N_2 (6 psi) to give a reaction atmosphere containing 80% H_2 and 20% N_2. The reaction mixtures were stirred (250 rpm) at ambient temperature (20 °C) for 2 h. After the desired reaction time the vessel was depressurized, the catalyst was removed via filtration and the remaining H_2O_2 quantified by UV/Vis spectroscopy.

Metal leaching studies

To provide an indication of the extent of metal leaching during the in-situ cyclohexane oxidation reaction, indicative model studies were conducted in the absence of the enzyme and substrate (*i.e.* under low-pressure H_2O_2 direct synthesis conditions) utilising 0.01 g of the heterogeneous catalyst (*i.e.* ten times that utilised for the cyclohexane oxidation reaction), with all other conditions as outlined as above. Post-reaction, the chemo-catalyst was removed via filtration and the reaction solution analysed by ICP-MS.

Unspecific peroxygenase preparation

Evolved AaeUPO (PaDa-I variant) designed in *Saccharomyces cerevisiae* was overproduced in *Pichia pastoris* in a bioreactor and purified to homogeneity (Reinheitszahl value [Rz] $[A_{418}/A_{280}] \sim 2.4$). Enzyme activities were determined using ABTS as substrate. Reactions were done in triplicate. 20 μL PaDa-I was added to 180 μL ABTS reaction mixture (100 mM sodium citrate-phosphate pH 4.4 with 0.3 mM ABTS and 2 mM H_2O_2) and substrate conversion was followed by measuring the absorption at 418 nm ($\varepsilon\, 418 = 36000\ M^{-1}\, cm^{-1}$). The PaDa-I concentration was appropriately diluted to give rise to linear enzyme kinetics. One unit is defined as the amount of enzyme that converts 1 μmol of substrate in 1 min.

Unspecific peroxygenase deactivation under reaction conditions

The effect of reaction conditions on the activity of the evolved AaeUPO (PaDa-I variant) were carried out in 50 mL gas tight round bottomed flasks rated to 60 psi and stirred using a Radleys 6 Plus Carousel equipped with a gas distribution system. Enzyme activities were determined using ABTS as substrate in a manner similar to that outlined above.

Note 4: The effect of cyclohexane oxidation reaction conditions on the activity of PaDa-I is reported in Table S5.

Catalytic testing of the tandem chemo-enzymatic system for cyclohexane oxidation

Reactions were carried out in 50 mL gas tight round bottomed flasks rated to 60 psi and stirred using a Radleys 6 Plus Carousel equipped with a gas distribution system. The reaction mixtures contained 15 $U mL_{RM}^{-1}$ PaDa-I (23 μL), 0.1 $mg\, mL_{RM}^{-1}$ of the metal catalyst (0.001 g) in potassium phosphate buffer (10 mL, 100 mM, pH 6, Merck) and cyclohexane (10 mM, Fischer Scientific). The catalysts were weighed directly into the glass vessels followed by the buffer solution. Immediately before starting the reactions, the enzyme and substrate were added. The sealed reaction vessels were pressurized to 29 psi with H_2 (23 psi) and air (6 psi) to give a reaction atmosphere containing 80% H_2 and 20% air. The reactions were stirred with a magnetic stirrer bar at 250 rpm at ambient temperature (20 °C) for 2 h, unless otherwise stated. After the desired reaction time product formation was monitored by extracting with 2×5 mL ethyl acetate containing 1-decanol (2 mM, Fischer Scientific) as the internal standard and subjecting aliquots of the organic layer to GC analysis (Agilent model 7658 equipped with a CP Wax 52 CB column). Additionally, the residual concentration of H_2O_2 was determined by UV/Vis spectroscopic analysis of the aqueous layer, as outlined above.

Cyclohexane conversion [Equation (3)] and product (cyclohexanol or cyclohexanone) selectivity [Equation (4)] were determined as follows:

$$\text{Cyxlohexane Conversion } (\%) = \frac{\text{mmol}_{\text{Cyclo (t(0))}} - \text{mmol}_{\text{Cyclo (t(1))}}}{\text{mmol}_{\text{Cyclo (t(0))}}} \times 100 \quad (3)$$

$$\text{Product Selectivity } (\%) = \frac{\text{mmol}_{\text{product (t(1))}}}{\text{mmol}_{\text{Cyclo (t(0))}} - \text{mmol}_{\text{Cyclo (t(1))}}} \times 100 \quad (4)$$

Further in-situ oxidation studies were carried out to determine the efficacy of using, pre-formed H_2O_2 at levels identical to those over a 2 h direct synthesis study (50 ppm), under identical conditions to those used above for in-situ cyclohexane oxidation. Notably, for these experiments, we have investigated both commercially supplied H_2O_2 (Merck) (*i.e.* in the presence of stabilisers) and that generated in our autoclave system (i.e. in the absence of stabilisers and utilising the aqueous buffered solution used for the enzymatic reactions).

Additional studies were conducted under individual gaseous reagents (H_2 and O_2 as air). In the case of those experiments conducted using commercial H_2O_2 a concentration of oxidant comparable to that formed if all the H_2 utilised in the in-situ approach was utilised, with total pressure fixed to 29 psi using N_2. For experiments using either H_2 or air alone total pressure was also maintained at 29 psi using N_2 in addition to the reagent gas.

To determine the role of leached metal species on process efficiency additional cyclohexane oxidation studies were conducted in the presence of the PaDa-I enzyme, and homogeneous metals at a concentration of active metals (as metal chlorides), far in excess of that present within the chemo-catalysed/enzymatic cascade reactions. In the case of these studies concentrations of precious metal salts comparable to that which would be present if 0.1% of metal species were leached from monometallic 1%Au/TiO_2, 1%Pd/TiO_2 and 1%Pt/TiO_2 catalysts, again using a catalyst mass ten times that utilised for our standard cascade reactions *(i.e.* 0.01 g). Such studies were conducted under an inert atmosphere (N_2, 29 psi) in the presence of preformed H_2O_2 (50 ppm, Merck) for 2 h, with all other conditions as outlined above.

In all cases the residual concentration of H_2O_2 was determined by UV/Vis spectroscopic analysis of the aqueous layer, as outlined above.

Catalyst reusability in the tandem chemo-enzymatic oxidation of cyclohexane, under low-pressure batch conditions

The performance of the metal catalysts was evaluated over multiple uses towards both the direct synthesis of H_2O_2 and cyclohexane oxidation in the tandem system. To obtain sufficient catalyst samples for testing over multiple uses, model reactions containing 0.05 g of chemo-catalyst and PaDa-I 15 (UmL_{RM}^{-1}), were conducted with reaction mixtures resemblant of the system at 30% cyclohexane conversion *i.e.* cyclohexane (7 mM) and cyclohexanol (3 mM), with all other conditions as outlined above. The spent catalyst was collected by vacuum filtration and washed with potassium phosphate buffer (2×5 mL, pH 6, 100 mM), before drying under vacuum (30 °C, 16 h). Aliquots of the dried sample (0.001 g) were then separately evaluated for activity towards H_2O_2 direct synthesis and in-situ cyclohexane oxidation. The procedure described above was repeated to allow for the evaluation of the chemo-catalyst upon third use. In a similar manner chemo-catalysts were subsequently utilised in the low-pressure direct synthesis of H_2O_2, after initial use on the tandem chemo-enzymatic oxidation reaction.

Evaluating efficacy towards the oxidation of cyclohexanol

The separate efficacy of the PaDa-I enzyme or the heterogeneous catalysts towards the oxidation of cyclohexanol was established in a similar manner to that used to determine activity of the chemo-enzymatic system towards cyclohexane oxidation, as outlined above.

The reaction mixtures contained 15 UmL_{RM}^{-1} PaDa-I (23 μL) or 0.1 $mg\,ml_{RM}^{-1}$ of the metal catalyst (0.001 g) in potassium phosphate buffer (10 mL, 100 mM, pH 6, Merck) and cyclohexanol (10 mM, Fischer Scientific). When using the heterogeneous catalyst, the materials were weighed out directly into the glass vessels followed by the buffer solution and substrate. The sealed reaction vessels were pressurized to 29 psi with H_2 (23 psi) and air (6 psi) to give a reaction atmosphere containing 80% H_2 and 20% air. The reactions were stirred (250 rpm) at ambient temperature (20 °C) for 2 h. After the desired reaction time product formation was monitored by extracting with 2×5 mL ethyl acetate containing 1-decanol (2 mM, Fischer Scientific) as the internal standard and subjecting aliquots of the organic layer to GC analysis (Agilent model 7658 equipped with a CP Wax 52 CB column).

A similar procedure to that outlined above was utilised when investigating the efficacy of the enzyme alone. However, in addition to the phosphate buffer and substrate, pre-formed H_2O_2 (50 wt.%, Merck) was also added, at a concentration comparable to that generated by the heterogeneous catalysts over a 2 h in-situ reaction (50 ppm). The sealed reaction vessels were pressurized to 29 psi with N_2 prior to stirring with a magnetic stirrer bar at 250 rpm at ambient temperature (20 °C) for 2 h. After the desired reaction time product formation was monitored by extracting with 2×5 mL ethyl acetate containing 1-decanol (2 mM, Fischer Scientific) as the internal standard and subjecting aliquots of the organic layer to GC analysis (Agilent model 7658 equipped with a CP Wax 52 CB column). The residual concentration of H_2O_2 was determined by UV/Vis spectroscopic analysis of the aqueous layer, as outlined above.

Catalyst Characterisation

Brunauer Emmett Teller (BET) surface area measurements were conducted using a Quadrasorb surface area analyser. A 5-point isotherm of each material was measured using N_2 as the adsorbate gas. Samples were degassed at 250 °C for 2 h prior to the surface area being determined by 5-point N_2 adsorption at −196 °C, and data analysed using the BET method.

The bulk structure of the catalysts was determined by powder X-ray diffraction using a (θ-θ) PANalytical X'pert Pro powder diffractometer using a Cu K_α radiation source, operating at 40 KeV and 40 mA. Standard analysis was carried out using a 40 min run with a back filled sample, between 2θ values of 10–80°. Phase identification was carried out using the International Centre for Diffraction Data (ICDD).

A Thermo Scientific K-Alpha$^+$ photoelectron spectrometer was used to collect XP spectra utilising a micro-focused monochromatic Al K_α X-ray source operating at 72 W. Data was collected over an elliptical area of approximately 400 μm^2 at pass energies of 40 and 150 eV for high-resolution and survey spectra, respectively. Sample charging effects were minimised through a combination of low energy electrons and Ar^+ ions, consequently this resulted in a C(1 s) line at 284.8 eV for all samples. All data was processed using CasaXPS v2.3.24 using a Shirley background, Scofield sensitivity factors and an electron energy dependence of −0.6 as recommended by the manufacturer.

DRIFTS measurements were taken on a Bruker Tensor 27 spectrometer fitted with a mercury cadmium telluride (MCT) detector. A sample was loaded into the Praying Mantis high temperature (HVC-DRP-4) *in-situ* cell before exposure to N_2 and then 1% CO/N_2 at a flow rate of 50 $cm^3 min^{<M-1}$. A background spectrum was obtained using KBr, and measurements were recorded every 1 min at room temperature. Once the CO adsorption bands in the DRIFT spectra ceased to increase in size, the gas feed was changed back to N_2 and measurements were repeated until no change in subsequent spectra was observed.

Aberration corrected scanning transmission electron microscopy (AC-STEM) was performed using a probe-corrected Hitachi HF5000 S/TEM, operating at 200 kV. The instrument was equipped with bright field (BF) and annular dark field (ADF) detectors for high spatial resolution STEM imaging experiments. This microscope was also equipped with a secondary electron detector and dual Oxford Instruments XEDS detectors (2×100 mm^2) having a total collection angle of 2.02 sr.

Metal leaching was quantified using an Agilent 7900 ICP-MS equipped with an I-AS auto-sampler using a 5-point calibration using certified reference materials from Perkin Elmer and certified internal standard from Agilent. All calibrants were matrix matched.

Acknowledgments

*The authors would like to thank the CCI-Electron Microscopy Facility which has been part-funded by the European Regional Development Fund through the Welsh Government, and The Wolfson Foundation. XPS data collection was performed at the EPSRC National Facility for XPS ('HarwellXPS'). **Funding:** A.S. R.J.L, J.B and G.J.H gratefully acknowledge Cardiff University and the Max Planck Centre for Fundamental Heterogeneous Catalysis (FUNCAT) for financial support. X.L. acknowledges financial support from National Key R&D Program of China (2021YFA1500300 and 2022YFA1500146) and National Natural Science Foundation of China (22072090 and 22272106). L.C. acknowledges the financial support from National Natural Science Foundation of China (21991153 and 21991150).*

Conflict of Interests

The authors declare no conflict of interest.

Data Availability Statement

The data that support the findings of this study are available in the supplementary material of this article.

Keywords: AuPdPt · cascade · hybrid catalysis · hydrogen peroxide · oxidation · peroxygenase

[1] I. Hermans, P. A. Jacobs, J. Peeters, *Chem. Eur. J.* **2006**, *12*, 4229–4240.
[2] E. L. Pires, J. C. Magalhães, U. Schuchardt, *Appl. Catal. A* **2000**, *203*, 231–237.
[3] U. Schuchardt, D. Cardoso, R. Sercheli, R. Pereira, R. S. da Cruz, M. C. Guerreiro, D. Mandelli, E. V. Spinacé, E. L. Pires, *Appl. Catal. A* **2001**, *211*, 1–17.
[4] Y. Wen, O. E. Potter, T. Sridhar, *Chem. Eng. Sci.* **1997**, *52*, 4593–4605.
[5] Y. Wang, D. Lan, R. Durrani, F. Hollmann, *Curr. Opin. Chem. Biol.* **2017**, *37*, 1–9.
[6] E. G. Hrycay, S. M. Bandiera, *Arch. Biochem. Biophys.* **2012**, *522*, 71–89.
[7] J. R. Scoville, I. A.Novicova (Cottrell Ltd.), US5900256, **1996**.
[8] Y. Ma, Y. Li, S. Ali, P. Li, W. Zhang, M. C. R. Rauch, S. J.-P. Willot, D. Ribitsch, Y. H. Choi, M. Alcalde, F. Hollmann, Y. Wang, *ChemCatChem* **2020**, *12*, 989–994.
[9] Y. Ma, P. Li, Y. Li, S. J. Willot, W. Zhang, D. Ribitsch, Y. H. Choi, R. Verpoorte, T. Zhang, F. Hollmann, Y. Wang, *ChemSusChem* **2019**, *12*, 1310–1315.
[10] V. Smeets, W. Baaziz, O. Ersen, E. M. Gaigneaux, C. Boissière, C. Sanchez, D. P. Debecker, *Chem. Sci.* **2020**, *11*, 954–961.
[11] P. N. R. Vennestrøm, E. Taarning, C. H. Christensen, S. Pedersen, J. Grunwaldt, J. M. Woodley, *ChemCatChem* **2010**, *2*, 943–945.
[12] F. Tieves, S. J. Willot, M. M. C. H. van Schie, M. C. R. Rauch, S. H. H. Younes, W. Zhang, J. Dong, P. Gomez de Santos, J. M. Robbins, B. Bommarius, M. Alcalde, A. S. Bommarius, F. Hollmann, *Angew. Chem. Int. Ed.* **2019**, *58*, 7873–7877; *Angew. Chem.* **2019**, *131*, 7955–7959.
[13] S. J. Freakley, S. Kochius, J. van Marwijk, C. Fenner, R. J. Lewis, K. Baldenius, S. S. Marais, D. J. Opperman, S. T. L. Harrison, M. Alcalde, M. S. Smit, G. J. Hutchings, *Nat. Commun.* **2019**, *10*, 4178.
[14] J. Brehm, R. J. Lewis, T. Richards, T. Qin, D. J. Morgan, T. E. Davies, L. Chen, X. Liu, G. J. Hutchings, *ACS Catal.* **2022**, 11776–11789.
[15] S. J. Freakley, Q. He, J. H. Harrhy, L. Lu, D. A. Crole, D. J. Morgan, E. N. Ntainjua, J. K. Edwards, A. F. Carley, A. Y. Borisevich, C. J. Kiely, G. J. Hutchings, *Science* **2016**, *351*, 965.
[16] D. A. Crole, R. Underhill, J. K. Edwards, G. Shaw, S. J. Freakley, G. J. Hutchings, R. J. Lewis, *Philos. Trans. R. Soc. A* **2020**, *378*, 20200062.
[17] P. Tian, F. Xuan, D. Ding, Y. Sun, X. Xu, W. Li, R. Si, J. Xu, Y. Han, *J. Catal.* **2020**, *385*, 21–29.
[18] S. Wang, D. E. Doronkin, M. Hähsler, X. Huang, D. Wang, J. Grunwaldt, S. Behrens, *ChemSusChem* **2020**, *13*, 3243–3251.
[19] J. K. Edwards, B. Solsona, E. N. Ntainjua, A. F. Carley, A. A. Herzing, C. J. Kiely, G. J. Hutchings, *Science* **2009**, *323*, 1037.
[20] F. Menegazzo, M. Manzoli, M. Signoretto, F. Pinna, G. Strukul, *Catal. Today* **2015**, *248*, 18–27.
[21] T. Richards, R. J. Lewis, D. J. Morgan, G. J. Hutchings, *Catal. Lett.* **2022**, *153*, 32–40.
[22] N. M. Wilson, P. Priyadarshini, S. Kunz, D. W. Flaherty, *J. Catal.* **2018**, *357*, 163.
[23] D. W. Flaherty, *ACS Catal.* **2018**, *8*, 1520.
[24] J. K. Edwards, J. Pritchard, L. Lu, M. Piccinini, G. Shaw, A. F. Carley, D. J. Morgan, C. J. Kiely, G. J. Hutchings, *Angew. Chem. Int. Ed.* **2014**, *53*, 2381–2384; *Angew. Chem.* **2014**, *126*, 2413–2416.
[25] J. W. M. Crawley, I.E. Gow, N. Lawes, I. Kowalec, L. Kabalan, C. R. A. Catlow, A. J. Logsdail, S. H. Taylor, N. F. Dummer, G. J. Hutchings, *Chem. Rev.* **2022**, *122*, 6795–6849.
[26] S. A. Kondrat, P. J. Miedziak, M. Douthwaite, G. L. Brett, T. E. Davies, D. J. Morgan, J. K. Edwards, D. W. Knight, C. J. Kiely, S. H. Taylor, G. J. Hutchings, *ChemSusChem* **2014**, *7*, 1326–1334.
[27] Y. Zhang, Q. Sun, G. Guo, Y. Cheng, X. Zhang, H. Ji, X. He, *Chem. Eng. J.* **2023**, *451*, 138867.
[28] T. Deguchi, H. Yamano, S. Takenouchi, M. Iwamoto, *Catal. Sci. Technol.* **2018**, *8*, 1002–1015.
[29] R. J. Lewis, K. Ueura, Y. Fukuta, S. J. Freakley, L. Kang, R. Wang, Q. He, J. K. Edwards, D. J. Morgan, Y. Yamamoto, G. J. Hutchings, *ChemCatChem* **2019**, *11*, 1673.
[30] X. Gong, R. J. Lewis, S. Zhou, D. J. Morgan, T. E. Davies, X. Liu, C. J. Kiely, B. Zong, G. J. Hutchings, *Catal. Sci. Technol.* **2020**, *10*, 4635.
[31] A. Santos, R. J. Lewis, G. Malta, A. G. R. Howe, D. J. Morgan, E. Hampton, P. Gaskin, G. J. Hutchings, *Ind. Eng. Chem. Res.* **2019**, *58*, 12623–12631.
[32] E. N. Ntainjua, J. K. Edwards, A. F. Carley, J. A. Lopez-Sanchez, J. A. Moulijn, A. A. Herzing, C. J. Kiley, G. J. Hutchings, *Green Chem.* **2008**, *10*, 1162.
[33] J. Li, T. Ishihara, K. Yoshizawa, *J. Phys. Chem. C* **2011**, *115*, 25359.
[34] L. Ouyang, G. Da, P. Tian, T. Chen, G. Liang, J. Xu, Y. Han, *J. Catal.* **2014**, *311*, 129–136.
[35] F. Gao, Y. Wang, D. W. Goodman, *J. Am. Chem. Soc.* **2009**, *131*, 5734–5735.
[36] F. Gao, D. W. Goodman, *Chem. Soc. Rev.* **2012**, *41*, 8009.

[37] J. K. Edwards, A. F. Carley, A. A. Herzing, C. J. Kiely, G. J. Hutchings, *Faraday Discuss.* **2008**, *138*, 225.
[38] R. J. Lewis, K. Ueura, Y. Fukuta, T. E. Davies, D. J. Morgan, C. B. Paris, J. Singleton, J. K. Edwards, S. J. Freakley, Y. Yamamoto, G. J. Hutchings, *Green Chem.* **2022**, *24*, 9496–9507.
[39] D. Wilbers, J. Brehm, R. J. Lewis, J. van Marwijk, T. E. Davies, D. J. Morgan, D. J. Opperman, M. S. Smit, M. Alcalde, A. Kotsiopoulos, S. T. L. Harrison, G. J. Hutchings, S. J. Freakley, *Green Chem.* **2021**, *23*, 4170–4180.
[40] G. J. Hutchings, C. J. Kiely, *Acc. Chem. Res.* **2013**, *46*, 1759.
[41] A. R. Wilson, K. Sun, M. Chi, R. M. White, J. M. LeBeau, H. H. Lamb, B. J. Wiley, *J. Phys. Chem. C* **2013**, *117*, 17557–17566.
[42] S. Wang, K. Gao, W. Li, J. Zhang, *Appl. Catal. A* **2017**, *531*, 89.
[43] L. Lan, H. Daly, Y. Jiao, Y. Yan, C. Hardacre, X. Fan, *Int. J. Hydrogen Energy* **2021**, *46*, 31054–31066.
[44] A. Karich, K. Scheibner, R. Ullrich, M. Hofrichter, *J. Mol. Catal. B* **2016**, *134*, 238–246.
[45] C. M. Crombie, R. J. Lewis, R. L. Taylor, D. J. Morgan, T. E. Davies, A. Folli, D. M. Murphy, J. K. Edwards, J. Qi, H. Jiang, C. J. Kiely, X. Liu, M. S. Skjøth-Rasmussen, G. J. Hutchings, *ACS Catal.* **2021**, *11*, 2701–2714.
[46] R. S. Heath, N. J. Turner, *Curr. Opin. Sustain. Chem.* **2022**, *38*, 100693.
[47] M. García-Bofill, P. W. Sutton, H. Straatman, J. Brummund, M. Schürmann, M. Guillén, G. Álvaro, *Appl. Catal. A* **2021**, *610*, 117934.
[48] M. A. F. Delgove, D. Valencia, J. Solé, K. V. Bernaerts, S. M. A. De Wildeman, M. Guillén, G. Álvaro, *Appl. Catal. A* **2019**, *572*, 134–141.
[49] A. P. Mattey, J. J. Sangster, J. I. Ramsden, C. Baldwin, W. R. Birmingham, R. S. Heath, A. Angeloastro, N. J. Turner, S. C. Cosgrove, S. L. Flitsch, *RSC Adv.* **2020**, *10*, 19501–19505.

Manuscript received: January 31, 2023
Revised manuscript received: April 4, 2023
Accepted manuscript online: April 13, 2023
Version of record online: ■■, ■■

RESEARCH ARTICLE

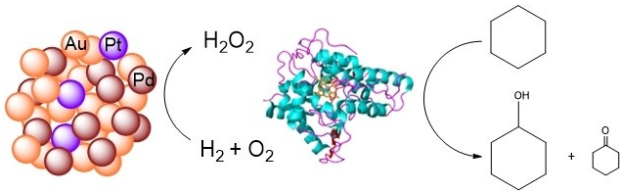

A. Stenner, Dr. R. J. Lewis, J. Brehm, T. Qin, Dr. Á. López-Martín, Dr. D. J. Morgan, Dr. T. E. Davies, Prof. L. Chen, Prof. X. Liu*, Prof. G. J. Hutchings**

Through the introduction of dopant levels of Pt into AuPd nanoparticles, the chemo-enzymatic oxidation of cyclohexane to KA oil (cyclohexanol and cyclohexanone) via in-situ H_2O_2 synthesis is significantly enhanced via the electronic modification of Pd species.